

Effect of Bi_2O_3 on the dynamics of Li^+ ions in $\text{Li}_2\text{O}\cdot\text{P}_2\text{O}_5$ glasses

Sonam Rani · Sujata Sanghi · Ashish Agarwal ·
Neetu Ahlawat

Received: 14 September 2008 / Accepted: 14 August 2009 / Published online: 29 August 2009
© Springer Science+Business Media, LLC 2009

Abstract Lithium ion transport has been studied in bismuth lithium phosphate glasses in the frequency range 20 Hz–1 MHz and in the temperature range 423–573 K using impedance spectroscopy. The addition of Bi_2O_3 in $\text{Li}_2\text{O}\cdot\text{P}_2\text{O}_5$ glass is related to the modification of the glass structure and facilitates the Li^+ ions migration. The ac and dc conductivities, activation energy of the dc conductivity and relaxation frequency are extracted from the impedance spectra. Conductivity of the present glass system is found to be ionic in nature. The electrical response of the glasses has been studied using both conductivity and electric modulus formalisms. A single ‘master curve’ for normalized plots of all the modulus isotherms observed for a given composition indicates the temperature independence of the dynamic processes for ions in these glasses. Nearly identical values of activation energy for dc conduction and for conductivity relaxation time indicate that the ions overcome same energy barrier while conducting and relaxing.

Introduction

Alkali phosphate glasses exhibit high ionic conductivity and have been studied extensively because of ease of formation, low melting point and strong glass-forming character [1]. Such glasses are potential candidates for energy storage devices and solid state batteries [2–4]. Oxide glasses containing Bi_2O_3 have also drawn much attention due to their high nonlinear optical susceptibility [5, 6]. Bi_2O_3 cannot form glass by itself like other traditional

glass formers; however, it can form glass in the presence of conventional glass formers [7]. In such glasses, high polarizing Bi(III) cation can reduce its coordination number from six to three and thus glass network may consist of both $[\text{BiO}_6]$ highly distorted octahedral and $[\text{BiO}_3]$ pyramidal units [8, 9]. Due to its dual role, as modifier with $[\text{BiO}_6]$ octahedral and as glass former with $[\text{BiO}_3]$ pyramidal units, bismuth ions may also influence the electrical properties of oxide glasses. Phosphate glasses possess low chemical durability, which can be increased by the addition of Bi_2O_3 through the formation of P–O–Bi bond [10, 11]. The effect of Bi_2O_3 on different properties of phosphate glasses has been investigated [12–16]. Shaim and Et-Tabirou [17] have investigated physical properties and electrical conductivity of sodium phosphate glasses containing 0–25 mol.% of Bi_2O_3 . The electrical conductivity of glasses depends upon their composition and to a considerable extent upon their structure and may be increased either by dissolving halides or by other salts in the glass structure [18, 19]. Further, when one network former progressively substitutes for another one, the conductivity of such mixed-former glasses exhibits different behaviours [19, 20]. The study of dielectric properties of glass materials helps in understanding their structure. Most of the disordered materials show a dielectric relaxation that is not described by an exponential (Debye-like) decay with a characteristic single decay time. The relaxation time in these materials follow a stretched exponential, the so-called Kohlrausch–Williams–Watts (KWW) function [21, 22]. The information of such stretched exponential relaxations is used to characterize the dynamics of ionic transport in ionically conducting disordered materials. In addition, the intrinsic disordered environment of charge carriers in glasses is believed to give rise to distinct transport mechanisms such as the usually observed

S. Rani · S. Sanghi · A. Agarwal (✉) · N. Ahlawat
Department of Applied Physics, Guru Jambheshwar University
of Science and Technology, Hisar 125001, Haryana, India
e-mail: aagju@yahoo.com

frequency dependent conductivity, $\sigma(\omega)$ [23]. The electrical conductivity of disordered materials is caused by at least two different contributions. First being thermal activation, in which the conductivity increases with temperature according to the Arrhenius law and second is by structural change of glass with composition [24]. Therefore, it is interesting to study the dynamic and relaxation mechanisms of the mobile ions in disordered ion conductors by interpreting the frequency dependent features in their dielectric response. In the present study, we have chosen binary $40\text{Li}_2\text{O}\cdot 60\text{P}_2\text{O}_5$ glass as the base material and partially replaced P_2O_5 by Bi_2O_3 to investigate the influence of Bi_2O_3 on the dynamic and relaxation mechanisms of lithium ions over a wide range of temperature and frequency by employing impedance spectroscopy.

Experimental

Glasses having composition $x\text{Bi}_2\text{O}_3\cdot(60-x)\text{P}_2\text{O}_5\cdot 40\text{Li}_2\text{O}$ (BP glasses), where $x = 0, 5, 10$ and 15 mol.%, were prepared using reagent grade chemicals Bi_2O_3 , Li_2CO_3 and $(\text{NH}_4)_2\text{HPO}_4$. Appropriate mixtures of these chemicals were preheated in a crucible for 5 h at 300°C to evaporate ammonia and water. Then the mixture was melted in an electrical muffle furnace at $1,100^\circ\text{C}$ for half an hour. The melts were then quickly quenched in between stainless steel plates. On quenching coin-shaped green-coloured samples were obtained. The melting has been carried out at higher temperature for ensuring the miscibility of the chemicals for the formation of glass. The glass samples were kept in desiccator to prevent possible attack by moisture. Glass samples of thickness $\sim 0.5\text{--}1.5$ mm were coated with silver paint on both sides and were annealed in

a furnace for 2 h at 200°C to remove the residual stresses before conductivity measurements. The electrical conductivity measurements were carried out by using an inductance analyzer (QuadTech 1910) from 20 Hz–1 MHz, with an applied potential of 1 V in the temperature range $150\text{--}300^\circ\text{C}$ (below glass transition temperature). The dc conductivity was calculated from Nyquist plots, where complex impedance data, $Z^*(\omega)$ were plotted in the complex plane ($Z'(\omega)$ vs. $Z''(\omega)$) at different temperatures.

Results

The Nyquist plots (at different temperatures) of the BP2 ($x = 5$ mol.%) glass sample consist of one semicircle with a characteristic spike (Fig. 1a) in low frequency region, which is due to the blocking electrode capacitance as the free mobile charges accumulate inside the sample surface and the electrode when samples have huge amount of mobile ions. All other glass samples also show similar behaviour. The spectra can be interpreted by equivalent electrical circuit with (inset in Fig. 1a) constant-phase element ($R\text{--}CPE$) of the sub circuit representing bulk contribution with parameters R_b and CPE_g , while CPE_{dl} represents blocking layer contribution. The necessity of using CPEs, rather than ordinary capacitors, is the consequence of the fact that the positions of the centres of the experimental circles are below the real axis of Nyquist plots [25, 26]. This suggests that the associated relaxation of ions is non-Debye in nature. The experimental impedance data were fitted to equivalent circuit with R and CPE_g in parallel. Values of equivalent circuit elements ($R_{at200^\circ\text{C}}$ and CPE_g) for all the glass samples are given in Table 1.

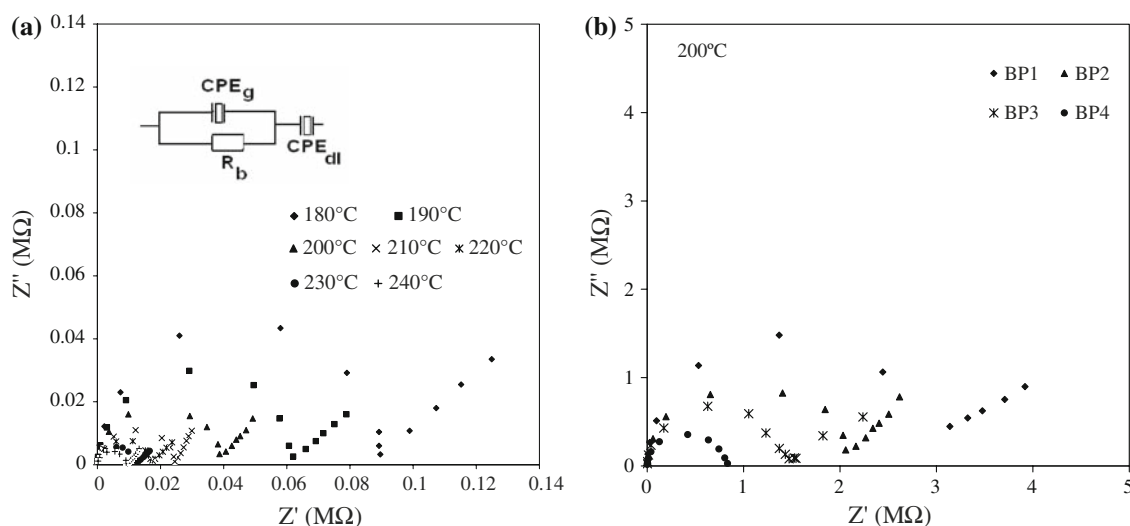


Fig. 1 a Experimental Nyquist plots for BP2 glass sample at different temperatures. *Inset*: equivalent circuit for impedance analysis. b Compositional dependence of normalized Nyquist plots at 200°C

Table 1 Equivalent circuit elements (R and C), activation energy for dc conductivity (E_{dc}), activation energy for conductivity relaxation time (E_r), stretched exponential parameter (β), concentration of Bi

ions and spacing between Bi ions (R_{Bi-Bi}) for the $x\text{Bi}_2\text{O}_3 \cdot (60 - x)\text{P}_2\text{O}_5 \cdot 40\text{Li}_2\text{O}$ glasses

| Sample code | x (mol.%) | $R_{at\ 200^\circ\text{C}}$ (M Ω) | CPE_g (10^{-10}F) | E_{dc} (eV) | E_r (eV) | β | Bi ions concentration (10^{22} ions cm^{-3}) | R_{Bi-Bi} (\AA) |
|-------------|-------------|---|---------------------------------------|---------------|------------|---------|---|------------------------------|
| BP1 | 0 | 0.16 | 1.272 | 0.94 | -0.90 | 0.84 | 0 | 0 |
| BP2 | 5 | 0.039 | 1.296 | 0.79 | -0.79 | 0.75 | 0.09 | 10.2 |
| BP3 | 10 | 0.088 | 1.127 | 0.86 | -0.80 | 0.79 | 0.21 | 7.81 |
| BP4 | 15 | 0.082 | 1.291 | 0.76 | -0.79 | 0.77 | 0.36 | 6.53 |

The dc resistance of each sample was obtained from the intersection of semicircle with the real axis at low frequency. Normalized Nyquist plots at 200 °C for all the glass samples are shown in Fig. 1b. This figure shows that the impedance curves shift towards origin of Nyquist diagram on addition of Bi_2O_3 into the base glass. The dc conductivity, σ_{dc} was calculated using the sample dimensions, and its reciprocal temperature dependence is shown in Fig. 2 for all the glass samples. σ_{dc} increases with increase in temperature and with increase in Bi_2O_3 content. Further, dc conductivity exhibits an Arrhenius-type temperature dependence given by the relation:

$$\sigma_{dc} = \sigma_0 \exp\left(-\frac{E_{dc}}{kT}\right). \tag{1}$$

The activation energy, E_{dc} was calculated from the least square straight line fitting of plots shown in Fig. 2, and the values for all the glass samples are given in Table 1. The ac conductivity of all the glass samples has been calculated from real and imaginary parts of the impedance data measured at various temperatures. Figure 3 shows frequency dependence of $\log \sigma(\omega)$ for BP2 glass sample at different temperatures, where $\sigma(\omega)$ is the total conductivity. The ac conductivity can be well approximated as:

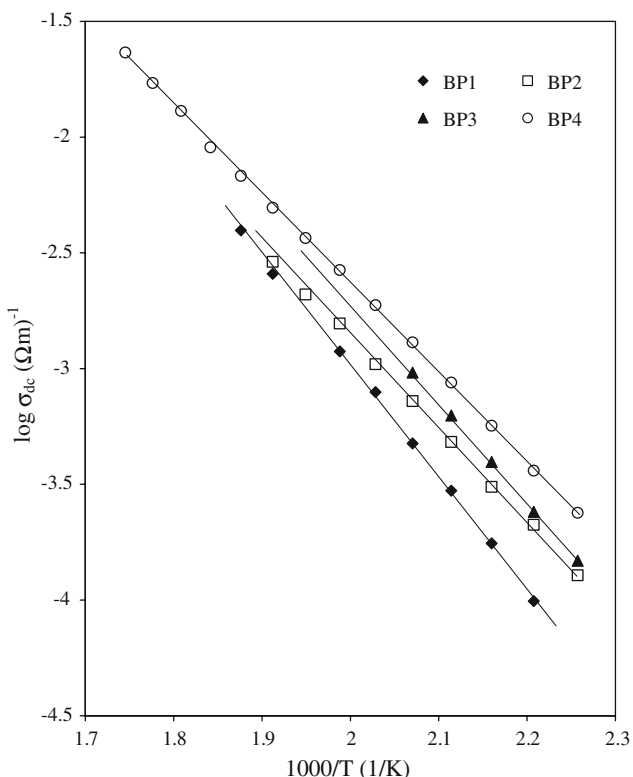


Fig. 2 Reciprocal temperature dependence of dc conductivity for all the glass samples

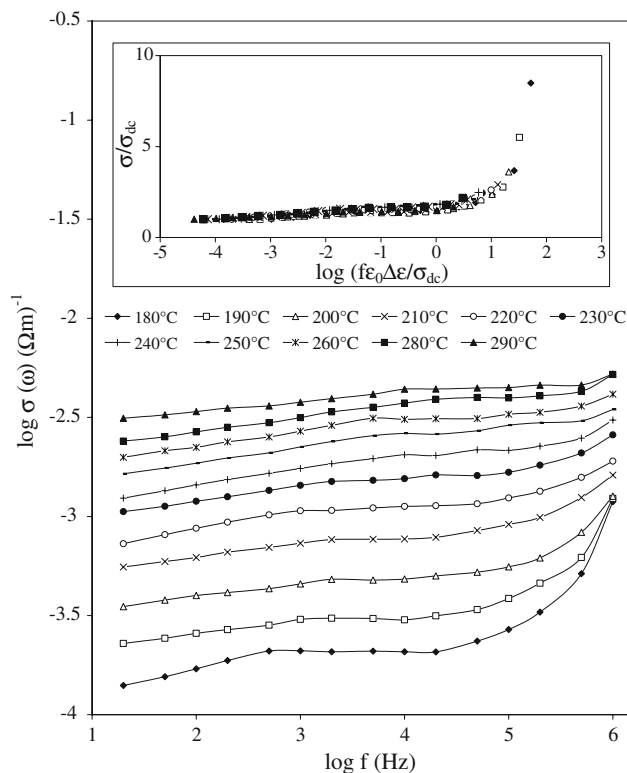


Fig. 3 Frequency dependence of conductivity for BP2 glass sample at different temperatures. *Inset:* the normalized conductivity isotherms for BP2 glass sample at the same temperatures as shown for conductivity

$$\sigma(f) = \sigma_{dc} \left[1 + \left(\frac{f}{f_h} \right)^s \right] + Af. \tag{2}$$

The first term (Jonscher term) in Eq. 2 results from the relaxation of dissociating ions in the glass matrix. f_h is a crossover frequency, which separates dc regime from the dispersive conduction. The frequency independent σ_{dc} results from the diffusion of ions at low frequency and is followed by a power law exponent ‘s’ and increases with increase in frequency. The last term in Eq. 2 represents an additional contribution to the conductivity due to processes that are believed to be unrelated to the cation motion [27, 28]. This contribution has been referred [29] to as the “near constant loss” (NCL) as its nearly linear frequency dependence implies a frequency independent dielectric loss. Figure 3 shows that with increase in temperature, f_h increases. It is also possible to scale the frequency dependent conductivity taken at different temperature into one single master curve. As the shape of conductivity curves does not depend on temperature, therefore, these curves can be superimposed by using Sidebottom Scaling [30].

An alternative formalism that may be used for analyzing the electrical response of glasses is the electrical modulus model. The electric modulus is defined as:

$$M^*(\omega) = 1/\varepsilon^* = M'(\omega) + iM''(\omega) \tag{3}$$

Figure 4 shows the frequency dependence of imaginary part of electrical modulus (M'') for BP2 glass sample at

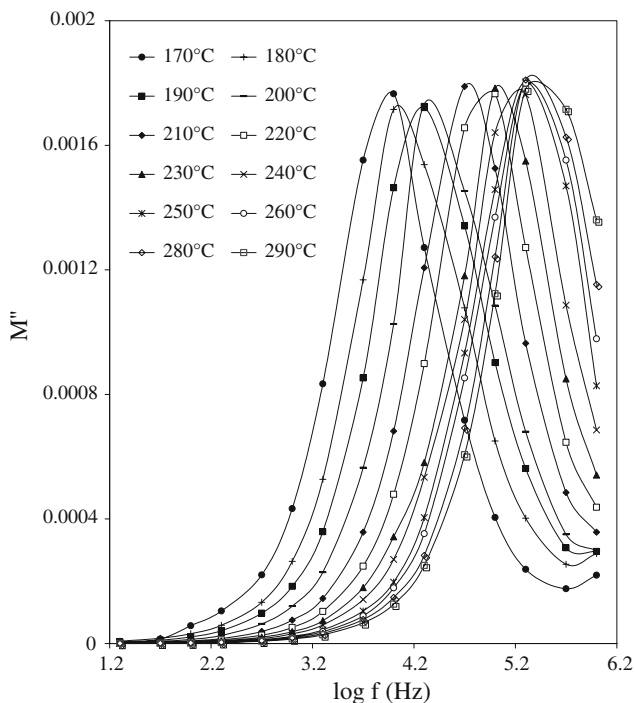


Fig. 4 Frequency dependence of the imaginary part of electric modulus (M'') at different temperatures for BP2 glass sample

different temperatures. The peak of these curves (M''_{max}) shifts to higher frequency with increasing temperature. The frequency region below M''_{max} determines the range in which charge carriers are mobile on long distances and for the frequency region beyond M''_{max} , the carriers are spatially confined to potential wells, being mobile on short distances making only localized motion within the wells. Figure 5 shows the conductivity and the normalized M'' spectra for BP1 and BP4 glasses at 210 °C. The low frequency dispersion in conductivity is associated with electrode polarization. From this figure, it can be seen that the maxima of M'' occur nearly in the middle of the conductivity crossover region [31]. Since $\varepsilon'_{\infty}(\omega)$ (ε'_{∞} is the high frequency permittivity value obtained from frequency dependence of ε' curves) increases with increase in Bi ions concentration, the M'' peak shifts towards higher frequency (Fig. 5). The characteristic frequency at which the maximum M'' occurs is used to evaluate the relaxation time $\tau_{M''}$ using the relation $\omega_{max} = 1/\tau_{M''} = \sigma_{dc}/(\varepsilon_0\varepsilon'_{\infty})$ [32]. Figure 6 shows the reciprocal temperature dependence of $\tau_{M''}$ and it satisfies the Arrhenius relation given by $\tau_{M''} = \tau_0 \exp(E_{\tau}/kT)$, where E_{τ} is the activation energy for the conductivity relaxation time. Values of E_{τ} have been calculated from the least square fitting of data in Fig. 6 and are given in Table 1. Figure 7 shows the normalized plots of modulus isotherms for BP2 glass sample, where the frequency axis is scaled by peak frequency f_m , M' axis is

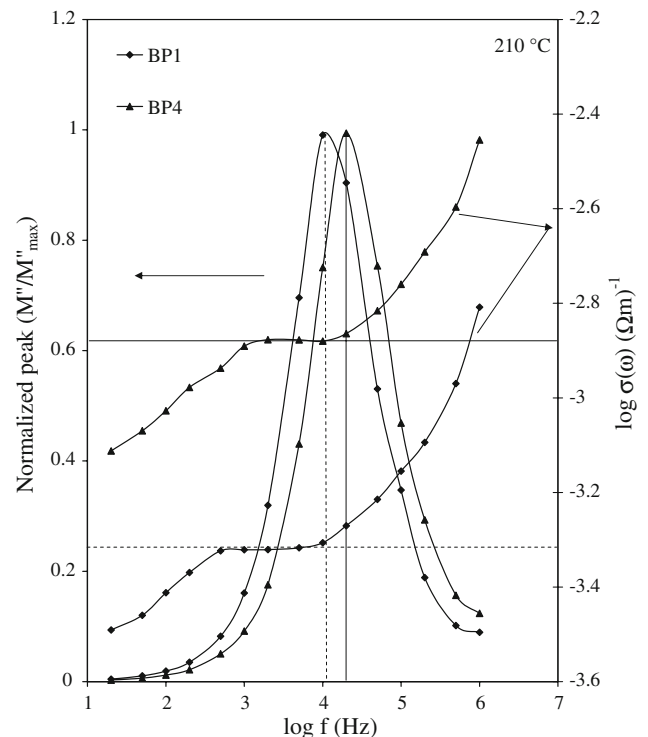


Fig. 5 Frequency dependence of normalized M'' and electrical conductivity $\sigma(\omega)$ for BP1 and BP4 glass samples at 210 °C

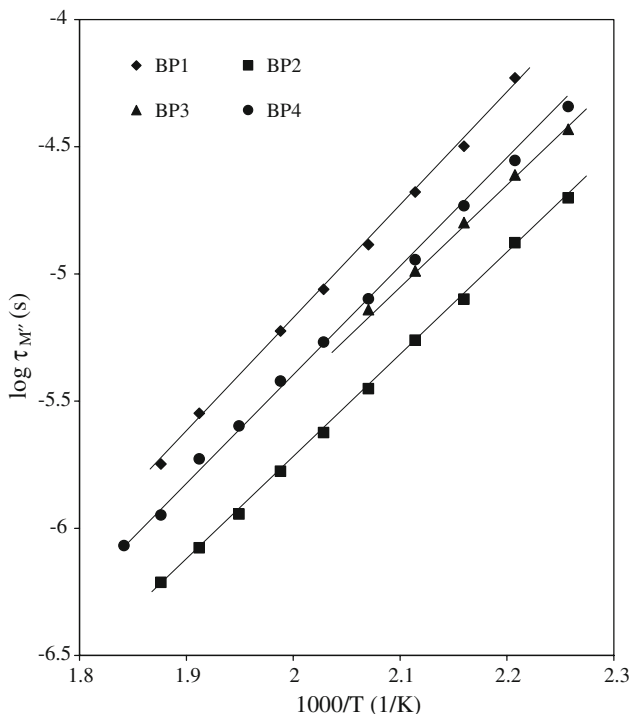


Fig. 6 Temperature dependence of the conductivity relaxation time ($\tau_{M''}$) for all the glass samples

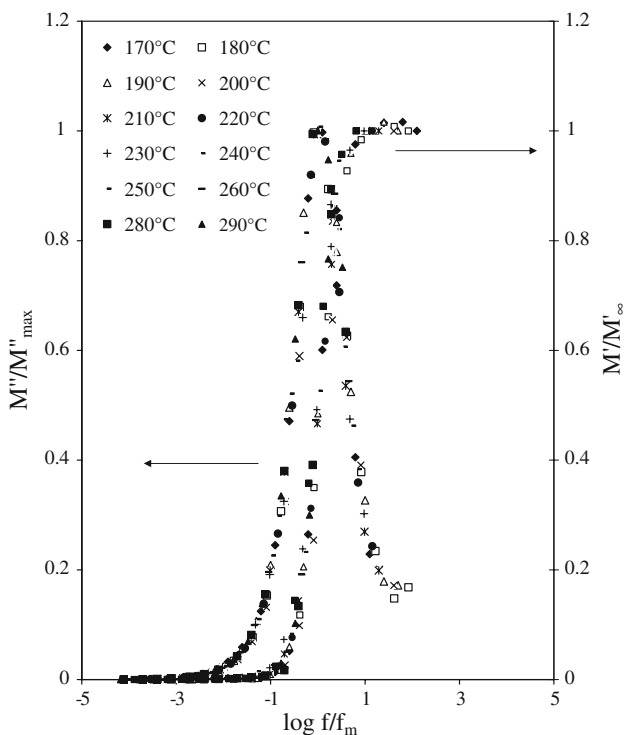


Fig. 7 Variations of M''/M'_∞ and M''/M''_{max} versus $\log(f/f_m)$ for BP2 glass at different temperatures

scaled by M'_∞ , and M'' axis is scaled by M''_{max} . A perfect overlapping of all the curves on a single master curve for all the temperatures can be observed.

Discussion

Nyquist plots (Fig. 1a) showing single semicircle indicate the single transport mechanism in the present glasses. Figure 1a, b show that the dc resistance decreases with increase in temperature and with increase in mol.% of Bi_2O_3 . The centre of these semicircles is depressed below the real axis suggesting that associated relaxation of ions is non-Debye in nature [26].

DC conductivity is enhanced on addition of Bi_2O_3 in the base glass (Fig. 2), which suggests that the glass structure is modified. As bismuth ions are more polarizable than phosphorous ions, therefore their presence in ionic network act as a polarizing unit facilitating the migration of Li^+ ions. It is also assumed that the addition of Bi_2O_3 increases the interstitial window without interrupting the P–O–P bonds present in the glass matrix allowing the Li^+ ions to pass through. It has also been reported that for low concentration of Bi_2O_3 in phosphate glasses the BiO_6 units are present, which acts as modifier and are ionic in nature [33, 34]. Hence contribution to total conductivity is two fold ionic in nature.

In conductivity formalism, for ionically conducting glasses, the real part of ac conductivity as a function of frequency is well approximated by Eq. 2. It is evident from Fig. 3 that the frequency dependence of conductivity in studied frequency window shows two distinct regimes: (i) the low frequency plateau corresponds to frequency independent conductivity, σ_{dc} , however, in this regime some dispersion can be seen, which is associated with the electrode polarization and (ii) high frequency dispersion regime. The switch over from the frequency independent region to frequency-dependent region is the signature of the onset of conductivity relaxation, which shifts towards higher frequency as the temperature increases. The dispersion behaviour in conductivity is attributed to the microscopic nature of inhomogeneities with the distribution of relaxation processes through distribution of energy barriers in the glass. The frequency independent conductivity may be attributed to the long-range transport of mobile ions in response to the electric field, where only successful diffusion contributes to dc conductivity. After applying the scaling law [30] for BP2 glass sample, the ac conductivity spectra obtained at different temperatures, collapse into one super curve (inset of Fig. 3), which suggests that the ionic conductivity mechanism is temperature independent. However, at low temperatures, the scaling appears to be weak in high frequency region. This observation shows the non-existence of the so-called ‘super scaling’ behaviour. The non-existence of super

scaling at low temperature is probably due to the NCL process in this region. The NCL regime is characterized by the almost linear frequency dependence of ac conductivity and weak temperature dependence. At a given temperature, NCL is observed for frequencies $\omega > \tau_m^{-1} = \omega_0 \exp(-E_m/kT)$. The crossover from NCL to ion hopping (i.e. NCL ceases when the ion diffusion starts) can be explained by above relation [35]. When the time scale for the diffusion of ions by hopping becomes comparable to or shorter than the time scale for the vibrational relaxation associated with the NCL process, the NCL process can no longer take place. Therefore, below the frequency or temperature defined by above relation, vibrational relaxation terminates and NCL ceases to exist and a well-defined crossover to ion hopping ac conductivity occurs.

The relaxation dynamics of mobile ions in bismuth lithium phosphate glasses has also been analyzed by electric modulus formalism for better description of the dynamic processes. The conductivity relaxation model, where a dielectric modulus is defined by $M^*(\omega) = 1/\varepsilon^*$, can provide information about the relaxation mechanism [32]. According to the previous discussion, two apparent relaxation regions appeared, the low frequency region, being associated with the hopping conduction and higher region being associated with the relaxation polarization process. When the data are presented in electrical modulus representation, the effect of electrode polarization can be avoided since the electrical modulus peaks, M'' , are shifted towards higher frequency (Fig. 4). From the comparison between crossover region of conductivity and maximum of M'' in Fig. 5 for BP1 and BP4 glasses, it can be seen that the position of maximum of M'' and the crossover point of conductivity is shifted to higher frequencies. If the glass is viewed as a composite made of microphases of different compositions and different relaxation times than the electrical current flows through the microheterogeneous structure made of different microphases in series. The asymmetric M'' originates from the nature of relaxation behaviour. This non-Debye behaviour of the M'' spectra can be related with the distribution of relaxation times. A variety of empirical functions, $\phi(t)$, have been used to describe the relaxation. The most widely used function is the KWW function. The relaxation of the quantity $\phi(t)$ is given by [21, 22]:

$$\phi(t) = \exp\left[-\left(\frac{t}{\tau}\right)^\beta\right] \quad (4)$$

where β is called the stretching exponent and its value lies between 0 and 1. When $\beta = 1$, the function represents simple exponential decay (Debye relaxation). Full width at half maximum values of M'' spectra are inversely correlated to the values of β . The calculated values of β for all the samples are temperature independent for a given

composition and vary from 0.75 to 0.84 for different compositions (Table 1). The perfect overlapping of normalized plots of modulus isotherms on a single master curve at different temperatures indicates that the dynamical processes are temperature independent (Fig. 7). This occurrence of a single master curve for all the isotherms also supports the temperature independence of the stretching exponential parameter β . Further, nearly close values of activation energy for dc conduction (E_{dc}) and conductivity relaxation (E_τ) for each glass composition (Table 1) suggests that the ions have to overcome the same barrier while conducting and relaxing. ' s ' and β often obey an empirical relation, $s + \beta = 1$ and this relation is used in Ngai's coupling model [36, 37]. However, this relation does not seem to be fit in the present study. There have been several attempts to correlate β to conductivity parameters like E_{dc} and inter-carrier-ion distance, R . In the present glasses, β is found to decrease with increasing concentration of Bi_2O_3 except BP2 glass sample (Table 1). This is in consonance with the coupling model, i.e. as the distance decreases, inter-cationic interaction increases, which slows τ and decreases β . In the present glass system, the value of β decreases with the increase of Bi_2O_3 content as the spacing between Bi ions decreases (Table 1). This indicates that the interaction between the mobile ions increases [38].

Conclusions

The electrical conductivity in present glasses increases with increase in Bi_2O_3 content and is ionic in nature due to the presence of Li^+ ions and BiO_6 octahedra in the glass matrix. The occurrence of super curve of electrical conductivity and master curve for electric modulus for a given composition indicates the temperature independence of the dynamic processes for ions in these glasses. The activation energy for relaxation time E_τ and for dc conduction E_{dc} are found to be very close to each other, which indicates that the dispersive conductivity $\sigma(\omega)$ originates from the migration of ions with same barrier while conducting as well as when relaxing. The non-exponential character of relaxation processes increases with decrease in β .

Acknowledgements The authors are thankful to All India Council for Technical Education, New Delhi for providing financial support. One of the authors (S.R.) is thankful to the Council for Scientific and Industrial Research, New Delhi for awarding Senior Research Fellowship (F. No.—09/752/(0015)/2008/EMR-I).

References

1. Martin SW (1991) J Am Ceram Soc 74:1767
2. Borsa F, Torgeson DR, Martin SW, Patel HK (1992) Phys Rev B 46:795

3. Chowdari BVR, Mok KF, Xie JM, Gopalakrisnan R (1995) *Solid State Ion* 76:189
4. Zafar M, Mausli A, Prasad PSS (1995) *Handbook of solid state batteries and capacitors*. World Scientific, New York
5. Deparis O, Mezzapesa FP, Corbari C, Kazansky PG, Sakaguchi K (2005) *J Non-Cryst Solids* 351:2166
6. Dumbaugh WH, Lapp JC (1992) *J Am Ceram Soc* 75:2315
7. Rawson H (1967) *Inorganic glass-forming systems*. Academic Press, London
8. Hazra S, Mandal S, Ghosh A (1997) *Phys Rev B* 56:8021
9. Baia L, Stefan R, Kiefer W, Popp J, Simon S (2002) *J Non-Cryst Solids* 303:379
10. Montagne L, Palavit G, Mairesse G (1996) *Phys Chem Glasses* 37:206
11. Montagne L, Palavit G, Mairesse G, Draoui M, Aomari K, Idrissi MS (1997) *Phys Chem Glasses* 38:15
12. Peng YB, Day DE (1991) *Glass Technol* 32:166
13. Ahaman Z, Et-tabirou M, Hafid M (1996) *Phase Trans* 56:247
14. Shaim A, Et-Tabirou M, Montagne L, Palavit G (2003) *Phys Chem Glasses* 44:26
15. Chahine A, Et-Tabirou M (2002) *Mater Res Bull* 37:1973
16. Chahine A, Et-Tabirou M, Pascal JL (2004) *Mater Lett* 58:2776
17. Shaim A, Et-Tabirou M (2003) *Ann Chim Sci Mater* 28:17
18. Ingram MD (1987) *Phys Chem Glasses* 28:215
19. Rodrigues ACM, Duclot MJ (1988) *Solid State Ion* 28–30:766
20. Minami T (1987) *J Non-Cryst Solids* 95/96:107
21. Kohlrausch R (1854) *Pogg Ann Phys Chem* 91:179
22. Williams G, Watts DC (1970) *Trans Faraday Soc* 66:80
23. Belmonte GG, Henn F, Bisquert J (2006) *Chem Phys* 330:113
24. Gowda VCV, Anavekar RC (2005) *Solid State Ion* 176:1393
25. Jonscher AK (1983) *Dielectric relaxation in solids*. Chelsea Dielectric Press, London
26. Barsoukov E, Macdonald JR (2005) *Impedance spectroscopy: theory, experiment and applications*. Wiley, New Jersey
27. Sidebottom DL, Green PF, Brow RK (1995) *Phys Rev Lett* 74:5068
28. Elliott SR (1994) *Solid State Ion* 70–71:27
29. Nowick AS, Vaysleyb AV, Kuskovsky I (1998) *Phys Rev B* 58:8398
30. Sidebottom DL (1999) *Phys Rev Lett* 82:3653
31. Sidebottom DL, Roling B, Funke K (2000) *Phys Rev B* 63:024301
32. Macedo PB, Moynihan CT, Bose R (1972) *Phys Chem Glasses* 13:171
33. Jiráček J, Koudelka L, Pospisil L, Mošner P, Montagne L, Delevoye L (2007) *J Mater Sci* 42:8592. doi:[10.1007/s10853-007-1848-7](https://doi.org/10.1007/s10853-007-1848-7)
34. Singh K (1996) *Solid State Ion* 93:147
35. Ngai KL (1999) *J Chem Phys* 110:10576
36. Ngai KL (1979) *Comments Solid State Phys* 9:127
37. Ngai KL, Rajagopal AK, Huang CY (1984) *J Appl Phys* 55:1714
38. Ngai KL, Rendell RW (2000) *Phys Rev B* 61:9393